

WheelMove-ID: Calculation details

Table of contents

WheelMove-ID: Calculation details	1
Introduction.....	2
1. Preprocessing.....	2
1.1. Realignment of IMUs frames	2
1.2. Computation of wheels angular velocities.....	5
1.3. Towards MWC linear and angular velocities	5
1.4. Correction of sliding / skidding.....	6
2. Tasks identification	6
2.1. Step 1: Piecewise Aggregate Approximation	6
2.2. Step 2: Symbolic Aggregate approximation (SAX)	7
2.3. Step 3: Logical search for locomotion task and symbolic representation	7
2.4. Step 4: Start and end refinement.....	8
2.5. Step 5: Reduction of variability.....	8
2.6. Step 6: Chronograms.....	8
3. References	9

Introduction

The WheelMove-ID application aims to assist in identifying the locomotion task performed during manual wheelchair (MWC) ambulation from measurement based on three inertial measurement units (IMU) placed on the rear wheels and the chassis. This document provides detailed explanations of the calculations implemented in WheelMove-ID.

It is organized around the two main steps:

- Preprocessing: calculation of linear and angular velocities of the MWC in the MWC reference frame.
- Task identification: identification, time frame by time frame, of the locomotion task performed.

The reference frames used throughout this document are defined in the figure below. All calculations and coordinate transformations assume these definitions.

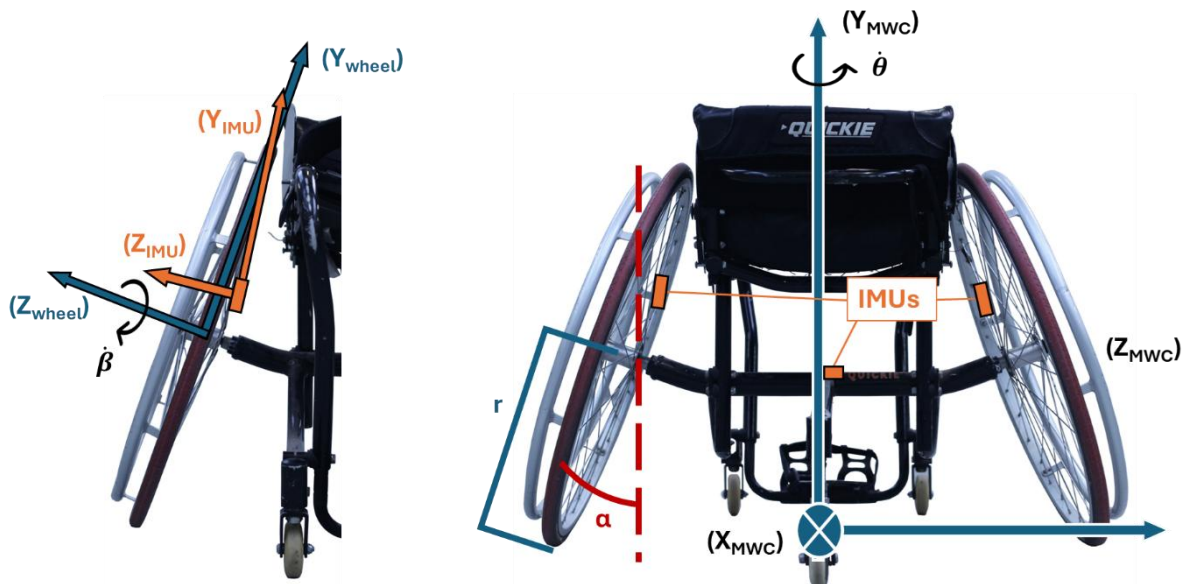


Figure 1: Reference frames used for computing MWC linear velocity from wheel-mounted IMUs. Left: front view; Right: rear view.

1. Preprocessing

Preprocessing enables the determination of MWC linear and angular velocities from accelerometer and gyroscope data. It consists of three main steps:

1. Realigning IMU frames to the MWC reference frame,
2. Computing each wheel's angular velocity,
3. Correcting sliding / skidding
4. Computing MWC linear and angular velocity from the previous step and MWC settings.

1.1. Realignment of IMUs frames

This step relies on calibration acquisitions for which the movement (or non-movement) of the MWC is known and controlled.

1.1.1. IMUs on the wheels

To realign the reference frames of the wheel-mounted IMUs, a short displacement during which an operator pushes the MWC in a straight line is recorded. This procedure makes it possible, for each wheel, to compute the transformation matrix $P_{R_{wheel}}^{R_{IMU}}$, and thus to re-express the gyroscope measurements originally expressed in the IMU reference frame in the wheel reference frame, whose axis $\overrightarrow{Z_{wheel}}$ is aligned with the wheel's axis of rotation:

$$(\overrightarrow{\Omega_{wheel/R_0}})_{R_{wheel}} = (\overrightarrow{\Omega_{imu/R_0}})_{R_{wheel}} = P_{R_{wheel}}^{R_{IMU}} (\overrightarrow{\Omega_{imu/R_0}})_{R_{IMU}} \quad (1.1)$$

That is,

$$P_{R_{IMU}}^{R_{wheel}} (\overrightarrow{\Omega_{imu/R_0}})_{R_{wheel}} = (\overrightarrow{\Omega_{imu/R_0}})_{R_{IMU}} \quad (1.2)$$

This transformation matrix results from two successive rotations: a first rotation, denoted γ , about the IMU axis $\overrightarrow{Y_{IMU}}$, followed by a second rotation, denoted ε , about the new axis $\overrightarrow{X'}$.

$$P_{R_{IMU}}^{R_{wheel}} = R_y R_x, \quad (1.3)$$

$$R_y = \begin{bmatrix} \cos \gamma & 0 & \sin \gamma \\ 0 & 1 & 0 \\ -\sin \gamma & 0 & \cos \gamma \end{bmatrix} \quad R_x = \begin{bmatrix} 1 & 0 & 0 \\ 0 & \cos \varepsilon & -\sin \varepsilon \\ 0 & \sin \varepsilon & \cos \varepsilon \end{bmatrix} \quad (1.4)$$

It can therefore be expressed as follows:

$$P_{R_{IMU}}^{R_{wheel}} = \begin{bmatrix} \cos \gamma & \sin \gamma \sin \varepsilon & \sin \gamma \cos \varepsilon \\ 0 & \cos \varepsilon & -\sin \varepsilon \\ -\sin \gamma & \cos \gamma \sin \varepsilon & \cos \gamma \cos \varepsilon \end{bmatrix} \quad (1.5)$$

Normalizing the gyroscope measurements transforms equation (1.2) into:

$$P_{R_{IMU}}^{R_{wheel}} \left(\frac{\overrightarrow{\Omega_{imu/R_0}}}{\|\overrightarrow{\Omega_{imu/R_0}}\|} \right)_{R_{wheel}} = \left(\frac{\overrightarrow{\Omega_{imu/R_0}}}{\|\overrightarrow{\Omega_{imu/R_0}}\|} \right)_{R_{IMU}} \quad (1.6)$$

Since the acquisition is performed during straight-line motion, dividing the wheel's rotational velocity by the norm of the angular velocities measured by the gyroscope yields a unit vector aligned with the wheel's axis of rotation $\overrightarrow{Z_{wheel}}$. Equation (1.6) therefore becomes:

$$P_{R_{IMU}}^{R_{wheel}} \begin{bmatrix} 0 \\ 0 \\ 1 \end{bmatrix} = \begin{bmatrix} \sin \gamma \cos \varepsilon \\ -\sin \varepsilon \\ \cos \gamma \cos \varepsilon \end{bmatrix} = \frac{1}{\|\overrightarrow{\Omega_{imu/R_0}}\|} \begin{bmatrix} \Omega_{x\,imu/R_0} \\ \Omega_{y\,imu/R_0} \\ \Omega_{z\,imu/R_0} \end{bmatrix} \quad (1.7)$$

Finally, equation (1.7) allows the identification of the angles ε and γ involved in the transformation matrix:

$$\gamma = \tan^{-1} \left(\frac{\Omega_x \text{imu}/R_0}{\Omega_z \text{imu}/R_0} \right) \quad (1.8)$$

$$\varepsilon = \tan^{-1} \left(\frac{-\Omega_y \text{imu}/R_0 \times \cos \gamma}{\Omega_z \text{imu}/R_0} \right) \quad (1.9)$$

Applying these angles to the transformation matrix ($P_{R_{wheel}}^{R_{IMU}}$) makes it possible to solve equation (1.1) and thus to re-express the gyroscope data in the wheel reference frame, whose axis $\overrightarrow{Z_{wheel}}$ corresponds to the effective axis of rotation of the wheel.

1.1.2. IMU on the MWC Frame

The realignment of the frame IMU is based on a static measurement of the gravitational acceleration vector in order to identify the transformation matrix $P_{R_{MWC}}^{R_{IMU}}$. This matrix allows the accelerometer data, measured in the IMU reference frame ($\overrightarrow{\Gamma_{imu/R_{imu}}} = \Gamma_x, \Gamma_y, \Gamma_z$), to be re-expressed in the MWC reference frame, whose vertical axis is defined by the gravitational acceleration vector \vec{g} :

$$(\overrightarrow{\Gamma_{imu/R_0}})_{R_{MWC}} = P_{R_{MWC}}^{R_{IMU}} (\overrightarrow{\Gamma_{imu/R_0}})_{R_{IMU}} \quad (1.10)$$

In the same manner as for the wheel-mounted IMUs, the transformation matrix $P_{R_{IMU}}^{R_{MWC}}$ is composed of two successive rotations about the axes $\overrightarrow{Y_{IMU}}$ and $\overrightarrow{X'}$, denoted σ and δ , respectively. It is expressed as:

$$P_{R_{IMU}}^{R_{MWC}} = \begin{bmatrix} \cos \sigma & \sin \sigma \sin \delta & \sin \sigma \cos \delta \\ 0 & \cos \delta & -\sin \delta \\ -\sin \sigma & \cos \sigma \sin \delta & \cos \sigma \cos \delta \end{bmatrix} \quad (1.11)$$

Next, by normalizing the accelerometer measurements by their norm (i.e., by the magnitude of the gravitational acceleration), Equation (1.10) becomes:

$$P_{R_{IMU}}^{R_{MWC}} \times \begin{bmatrix} 0 \\ 0 \\ -1 \end{bmatrix} = \frac{(\overrightarrow{\Gamma_{imu/R_0}})_{R_{IMU}}}{\|\overrightarrow{\Gamma_{imu/R_0}}\|} \quad (1.12)$$

That is,

$$\begin{bmatrix} -\sin \sigma \cos \delta \\ \sin \delta \\ -\cos \sigma \cos \delta \end{bmatrix} = \frac{1}{\|\overrightarrow{\Gamma_{imu/R_0}}\|} \begin{bmatrix} \Gamma_x \\ \Gamma_y \\ \Gamma_z \end{bmatrix} \quad (1.13)$$

Finally, Equation (1.13) enables the identification of the angles σ and δ involved in the transformation matrices:

$$\sigma = \tan^{-1} \left(\frac{\Gamma_x}{\Gamma_z} \right) \quad (1.14)$$

$$\delta = \tan^{-1} \left(\frac{-\Gamma_y \times \cos \sigma}{\Gamma_z} \right) \quad (1.15)$$

Injecting these angles into the transformation matrices allows Equation (1.10) to be solved. This equation makes it possible to re-express the data from the IMU mounted on the MWC frame in the MWC reference frame, whose axis $\overrightarrow{Z_{MWC}}$ is defined by the gravitational acceleration and oriented upward.

This correction is based on two vectors defining the horizontal plane and one vector defining the vertical direction. For this reason, no orientation error about the resulting vertical axis can be corrected. Correct alignment of the IMU \vec{X} axis with the MWC sagittal plane is therefore of critical importance.

1.2. Computation of wheels angular velocities

As thoroughly described by **Pansiot et al. 2011** and **Poulet et al. 2023**, the computation of wheels angular velocities from an IMU aligned with the wheel reference frame depends on the rear wheel camber angle (α) and follows this equation:

$$\dot{\beta} = \Omega_z \pm \sqrt{\Omega_x^2 + \Omega_y^2} \tan \alpha \quad (1.16)$$

Where Ω_i represents the gyroscope data around the i -axis, with z-axis being the axis rotation of the wheel.

1.3. Towards MWC linear and angular velocities

The following equation provides MWC linear velocity along its anteroposterior axis from both wheels' angular velocity ($\dot{\beta}$) and radius (r), assuming that the wheels are rolling without slipping.

$$V_x = \left(\frac{\dot{\beta}_{left\ wheel} \cdot r_{left\ wheel} \mp \dot{\beta}_{right\ wheel} \cdot r_{right\ wheel}}{2} \right) \quad (1.17)$$

Similarly, the following equation provides MWC angular velocity around its vertical axis from both wheel's angular velocity ($\dot{\beta}$), radius (r) and from the distance between the geometric center of rotation of each wheel (d), assuming that the wheels are rolling without slipping.

$$\dot{\theta} = \frac{(\dot{\beta}_{left\ wheel} \cdot r_{left\ wheel} - \dot{\beta}_{right\ wheel} \cdot r_{right\ wheel})}{d} \quad (1.18)$$

Because the assumption of rolling without slipping is not always satisfied, particularly during athletic movements, a correction algorithm is applied to the linear velocity of the MWC.

Thanks to the realignment procedure applied to the IMU mounted on the MWC frame, the angular velocity of the MWC can be directly measured from this sensor without relying on the rolling-without-slipping assumption:

$$\dot{\theta} = \Omega_{z \text{ imu}_frame} \quad (1.19)$$

1.4. Correction of sliding / skidding

The algorithm first identifies periods of slipping by comparing the MWC's angular velocity computed from the wheel-mounted IMU using equation (1.18), which is sensitive to slipping, with the angular velocity measured by the frame-mounted IMU, which is insensitive to slipping. Slipping is considered detected when the absolute difference between these two signals exceeds a threshold of 0.2 rad/s.

Next, the MWC's linear speed is corrected individually for each slipping episode lasting more than 6 time frames. For this, the MWC linear speed is replaced by the time integration of the acceleration measured along the forward axis of the frame-mounted IMU. Adjustments are applied to align the integrated signal with the MWC velocity immediately before and after the slipping interval.

2. Tasks identification

The task identification process is adapted from **Deves et al. 2024** and relies on the analysis of four signals:

- The wheelchair linear velocity (V_x) [in m/s], more especially, the velocity of the midpoint between both rear wheels' centers
- The absolute value of wheelchair linear velocity ($\text{abs}(V_x)$) [in m/s]
- The absolute value of the angular velocity ($\text{abs}(\dot{\theta})$) of the wheelchair around the vertical axis [in °/s]
- The wheelchair curvature radius (R), expressed in the MWC coordinate system and aligned with the line passing through the centers of the rear wheels, under the condition of rolling without slipping of both rear wheels [in m]. It is derived from the following equation, which is based on linear and angular velocities.

$$R = \text{abs}\left(\frac{V_x}{\dot{\theta}}\right) \quad (2.1)$$

The purpose of the algorithm is to provide a symbolic representation of displacement that highlights the different locomotion tasks performed, more specifically the static phase, forward propulsion, backward propulsion, pivot rotation, tight rotation, and wide rotation. Rotations are detected independently of their directions, but this could easily be implemented by further processing based on the sign of $\dot{\theta}$.

2.1. Step 1: Piecewise Aggregate Approximation

The four signals mentioned above are first transformed into segments using Piecewise Aggregate Approximation (PAA). This step reduces computational requirements and, more importantly, smooths the data, thereby minimizing the risk of versatility in task detection. The duration of each

segment is user-defined through the **Segmentation duration (s)** parameter. The algorithm was developed and tested using a segmentation duration of 0.25s presented as default value.

As a result, segmentation may slightly reduce the precision in determining the exact frame at which a task begins and finishes. To mitigate this effect, PAA is applied multiple times with temporal offsets ranging from 1 to n frames, n corresponding to the number of acquisition frames in a segment.

This step results in four n by m matrices, one for each of the 4 signals studied, with m corresponding to the total number of frames.

2.2. Step 2: Symbolic Aggregate approximation (SAX)

The values in the four matrices are then replaced by logical values based on user-defined thresholds. This transformation resulted in the four signals being converted into matrices of logical values ("a", "b", and "c").

Table 1: Default thresholds.

Signal	a	b	c
V_x (m/s)	≤ -0.5	$-0.5 < v < 0.5$	≥ 0.5
$abs(V_x)$ (m/s)		< 0.5	≥ 0.5
$abs(\dot{\theta})$ (°/s)		< 40	> 40
R (m)	≤ 0.2	$0.2 < R < 0.5$	≥ 0.5

Then, in order to circle back to a single vector per signal, the most represented logical value per time frame (among the n series due to temporal offsets) is retained.

This yields four logical vectors representing the MWC state for each signal, referred to as SAX signals.

2.3. Step 3: Logical search for locomotion task and symbolic representation

The values of the 4 SAX signals are then search frame by frame for pattern identification using the following table:

Table 2: Identification of locomotor tasks based on SAX signal and pattern identification

V_x	c	a				
$abs(V_x)$	b	c	c			
$abs(\dot{\theta})$	b	b	b	c	c	c
R				a	b	c
Task identified	Static	Forward propulsion	Backward propulsion	Pivot rotation	Tight rotation	Wide rotation

The resulting unique signal is as long as the initial signals (m frames) and is composed solely of logical values (here capital letters) representing locomotor tasks.

2.4. Step 4: Start and end refinement

Some of the default thresholds values presented in Table 1 are intentionally set relatively high to avoid detecting non-locomotor movements that do not correspond to actual locomotion tasks. For example, forward propulsion is only considered when the linear velocity exceeds 0.5 m/s.

An additional processing step using complementary thresholds is therefore introduced to help identify the true onset of locomotor tasks. For instance, the default complementary thresholds are set to 0.1 m/s for linear velocity and to 10 °/s for angular velocity. This additional step relies on the transitions initially identified: from each transition, the signal is read in both forward and backward directions to verify whether the complementary threshold is effectively reached, allowing a more accurate localization of the task onset. During this refinement stage, newly defined thresholds related to turning events are given priority over thresholds associated with other locomotor tasks.

This approach enables a more accurate refinement of the start and end frames of locomotor tasks, while preventing the noise that would result from lowering the initial detection thresholds.

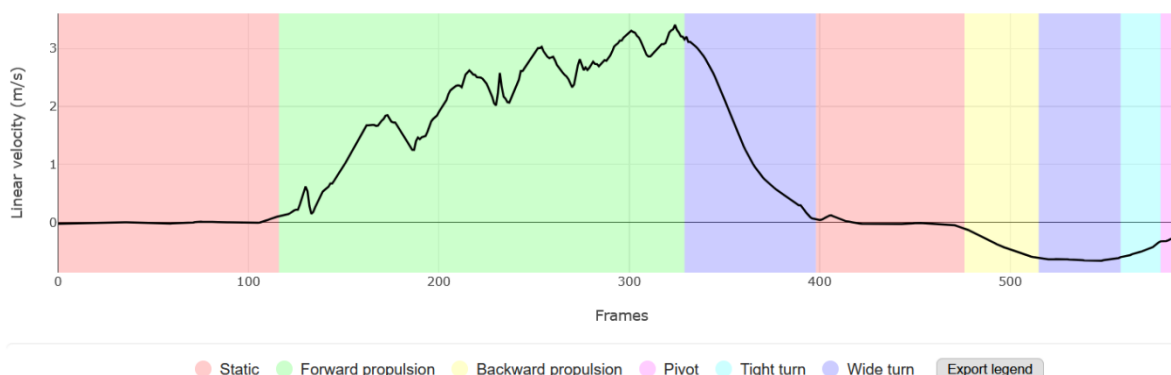
2.5. Step 5: Reduction of variability

The resulting combined signal may still exhibit undesired fluctuations in the identified tasks, particularly when signal values are close to the detection thresholds. To reduce this variability, a final post-processing step is applied: any isolated task shorter than the segmentation duration that is preceded and followed by the same task is replaced by that surrounding task.

For instance, if the algorithm detected several consecutive segments of straight-line movement, but a single short segment of wide turn appeared in between, that wide turn would be transformed into a straight-line frame.

2.6. Step 6: Chronograms

Finally, chronograms are a simple way to present the results, with each color representing a locomotor task.



3. References

- Pansiot**, J., Z. Zhang, B. Lo, and G. Z. Yang. 2011. "WISDOM: Wheelchair Inertial Sensors for Displacement and Orientation Monitoring." *Measurement Science and Technology* 22(10):105801. doi:[10.1088/0957-0233/22/10/105801](https://doi.org/10.1088/0957-0233/22/10/105801).
- Poulet**, Yoann, Florian Brassart, Emeline Simonetti, Hélène Pillet, Arnaud Faupin, and Christophe Sauret. 2022. "Analyzing Intra-Cycle Velocity Profile and Trunk Inclination during Wheelchair Racing Propulsion." *Sensors* 23(1):58. doi:[10.3390/s23010058](https://doi.org/10.3390/s23010058).
- Deves**, Mathieu, Christophe Sauret, Ilona Alberca, Lorian Honnorat, Yoann Poulet, Arnaud Hays, and Arnaud Faupin. 2024. "Activity Identification, Classification, and Representation of Wheelchair Sport Court Tasks: A Method Proposal." *Methods and Protocols* 7(5):84. doi:[10.3390/mps7050084](https://doi.org/10.3390/mps7050084).